

FIRST EXPERIMENTAL RESULTS OF LARGE SCALE DEBRIS BED REFLOOD TESTS IN THE PEARL FACILITY

Nourdine Chikhi*, T. Garcin, F. Foubert, P. March and F. Fichot

IRSN French Nuclear Safety Institute,
Cadarache Nuclear Center, BP 3,
13115 Saint-Paul-lez-Durance, France

ABSTRACT

During a severe accident in a nuclear power plant, the degradation of fuel rods and melting of materials lead to the accumulation of core materials, which are commonly, called "debris beds". To stop core degradation and avoid the reactor vessel rupture, the main accident management procedure consists in injecting water. In the case of debris bed, the reflooding models used for Loss of Coolant Accident are not applicable. The IRSN has launched an experimental program on debris bed reflooding to develop new models and to validate severe accident codes. The PEARL facility has been designed to perform, for the first time, the reflooding of large scale debris bed ($\varnothing 540\text{mm}$, $h=500\text{mm}$ and 500kg of steel debris) in a pressurized containment. The bed is heated by means of an induction system. A specific instrumentation has been developed to measure the debris bed temperature, pressure drop inside the bed and the steam flow rate during the reflooding. In this paper, the results of the first integral reflooding tests performed in the PEARL facility at atmospheric pressure up to 700°C are presented. Focus is made on the quench front propagation and on the steam flow rate during reflooding. The effect of water injection flow rate, debris initial temperature and residual power are also discussed. Finally, an analytical model providing the steam flow rate and the quench front velocity is proposed to interpret these results.

KEYWORDS

Reflooding, Debris Bed, Severe Accident, PEARL

1. INTRODUCTION

In case of a hypothetical severe accident in a pressurized water reactor (PWR), the degradation of fuel rods and melting of materials lead to the accumulation of core materials, which are commonly, called "debris beds". There are two main possible configurations of debris beds. The first configuration of the debris bed may result from the quenching of very hot rods during the reflooding of the core: this was observed in TMI-2 reactor above the core molten pool, with debris size of the order of several millimeters [1]. The second configuration may result from the fragmentation of jets of molten material falling through water in the lower plenum of the vessel: this was observed in many experimental facilities [2, 17, 18], and the average debris size is of the order of a few millimeters [2]. The coolability of debris beds has been the subject of numerous questions and studies in the last thirty years: some of them are recalled below. Many experimental studies and theoretical models have focused on the determination of the "dry-out" heat flux, i.e. the maximum volumetric power that can be removed from a debris bed by water. In most cases, one-dimensional debris beds were considered [3]. It was usually considered that a non-coolable debris bed

* Corresponding author: nourdine.chikhi@irsn.fr

would quickly rise in temperature, due to the residual decay heat, then melt and form a large pool of superheated oxides and metals that would expand even when surrounded by water. But it was also observed later that local thermal equilibrium may not exist everywhere in the debris bed, even for heated debris covered by water at saturation temperature (SILFIDE experiment, [4]). The flow of overheated steam through the bed appears as a relatively important process to cool the “dry” debris, leading to situations that are coolable even though the debris bed is dry in some places. On the other hand, the reflooding of hot debris beds has received less attention because it was considered that coolability was the main issue for debris beds. However, some experimental results are available [5, 6, 7, 8, 9] and a few models have been proposed [8, 10, 11]. In the case of reflooding, the existence of large temperature differences between the solid particles, the water and the steam makes modeling and experimental measurements very difficult, which may also explain why it was less studied. Furthermore, flow patterns are complex since, for very high temperature particles, steam becomes the “wetting” phase due to the presence of a stable steam film around the particles. This was observed experimentally, on single spheres, by Dhir and Purohit [12].

Models may be divided into two categories: 0D/1D models which are able to provide global parameters (outlet steam flow rate, quench front velocity, etc.) and 2D/3D models which provide detailed flow fields (void fraction, velocities, etc.). Similarly, experimental data can provide global parameters but may also be used for validation of 2D/3D codes when local measurements are available. But, in general, because of the lack of accurate local measurements in debris beds, models must rely on several assumptions. In the case of debris bed, the reflooding models used for Loss of Coolant Accident (LOCA) are not applicable. That is why the “Institut de Radioprotection et de Sûreté Nucléaire” (IRSN), has launched an experimental program on debris bed reflooding, called PEARL, to develop new reflooding models and to validate 2D/3D models. The aim is to predict the consequences of the water reflooding of a severely damaged reactor core where a large part of the core has collapsed and formed a debris bed.

In this paper, new results on reflooding are presented. They have been obtained in a large scale debris bed (PEARL facility, Ø540mm, h=500mm and 500kg of stainless steel spherical particles) heated with a volumetric heat source (induction). This experiment is the first of its kind at such scale. A special attention was paid to the instrumentation to accurately measure debris bed temperature, pressure drop inside the bed and the steam flow rate during the reflooding. The progression kinetics of water within the bed, the timing of quenching and the “conversion ratio” (which is the steam flow rate produced divided by the water injection flow rate) can be deduced from these measurements. One specific feature of the PEARL facility is the presence of a lateral by-pass in order to simulate the presence of non-damaged zones at the periphery of the bed. This by-pass induces flow patterns which differ significantly from previously observed patterns in 1D experiment.

After a description of the PEARL facility and its instrumentation, the main experimental results are presented and discussed. Tests are made at atmospheric pressure, with water injection from the bottom. Volumetric power is maintained during reflooding. Its effect is visible in some tests and is discussed. In the final part, a model is proposed to interpret the result, in particular the conversion ratio. The model also provides indications about the effect of the bypass.

2. THE PEARL FACILITY

2.1. The PEARL thermal-hydraulic loop

The PEARL facility (Fig.1) has been designed to simulate large scale debris bed reflooding under pressure. The debris bed is supported by a bed made of 8mm quartz balls and positioned in a quartz tube (test section, Fig.2). It is heated by an induction coil linked to a high frequency generator. The quartz tube is placed in a stainless steel sealed (up to 10bar) containment. Water enters the test section by the bottom or the top from a pressurized water tank. In the water injection line, the water flow rate is measured with a Coriolis flow meter and regulated by an electro-pneumatic valve. The steam, generated by reflooding, flows from the test section outlet at the top through a heated steam line equipped with a steam flow meter

(Annubar flow meter). The steam line is ended by a pneumatic valve which regulates the pressure in the test section. This line is temperature-controlled so that condensation of steam is avoided.

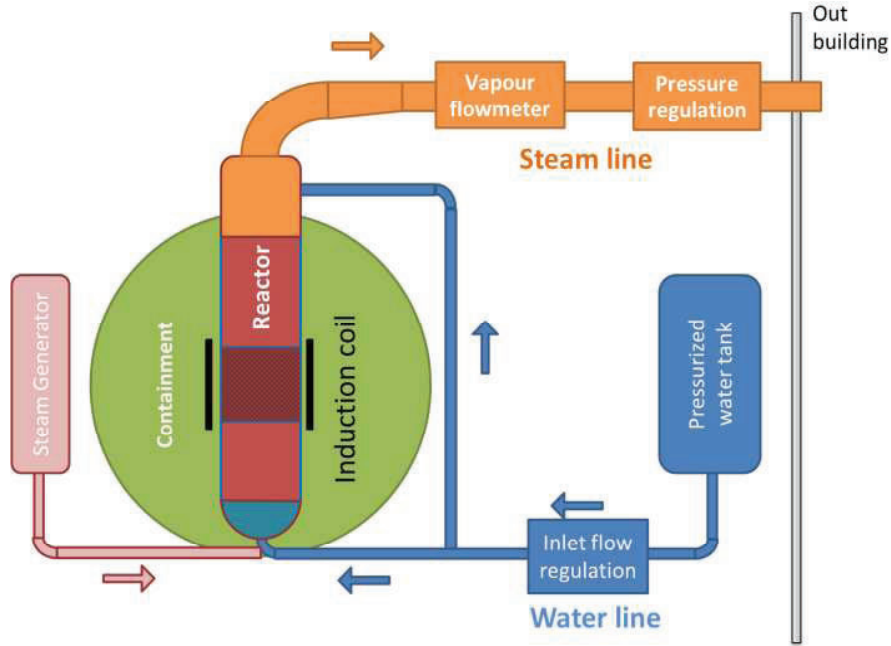


Figure 1. Schematic view of the PEARL facility.

2.2. The PEARL test section

The PEARL test section is composed of a quartz tube 2.6m long (internal diameter=540mm, thickness=10mm). The experimental debris bed has a cylindrical shape, approximately 500mm in height and 450mm in diameter. The bed is made of 4mm stainless steel balls. It is surrounded by a bypass made of 8mm quartz balls. A quartz ball bed, 100mm in height, is supporting the experimental debris bed so that it is well positioned according to the induction coil position.

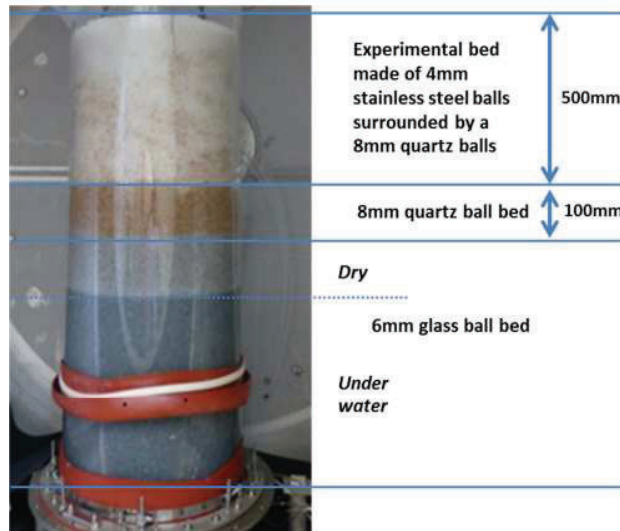


Figure 2. PEARL test section

2.3. The PEARL test conduct

The main phases of a PEARL test are shown on Fig. 3 and summarized in this section. At the beginning, the test section including the experimental debris bed is at room temperature. The steam line is pre-heated at 120°C. The bed heat-up consists of several separate phases. First, an approximately 20 kg/h steam flow rate is injected through the test section from the bottom in order to heat up the by-pass quartz balls. At the same time starts the first heat-up phase (150W/kg) of the bed. When the bed temperature reaches 150°C, the furnace is stopped. During the stabilization phase, the steam generator goes on until the bypass quartz ball temperature is equal to the saturation temperature (100°C at atmospheric pressure). Then, the second heat-up phase (150W/kg) increases the bed temperature. When the target temperature T_{ini} is reached, the furnace is stopped again and the water is injected from the pressurized water tank. The furnace is restarted as water penetrates the bottom of the experimental bed. The Annubar flow meter detects the start of steam production. The bed is cooled down. The water injection and the furnace are definitely stopped when the temperature of the bed (every thermocouple) is below the saturation temperature.

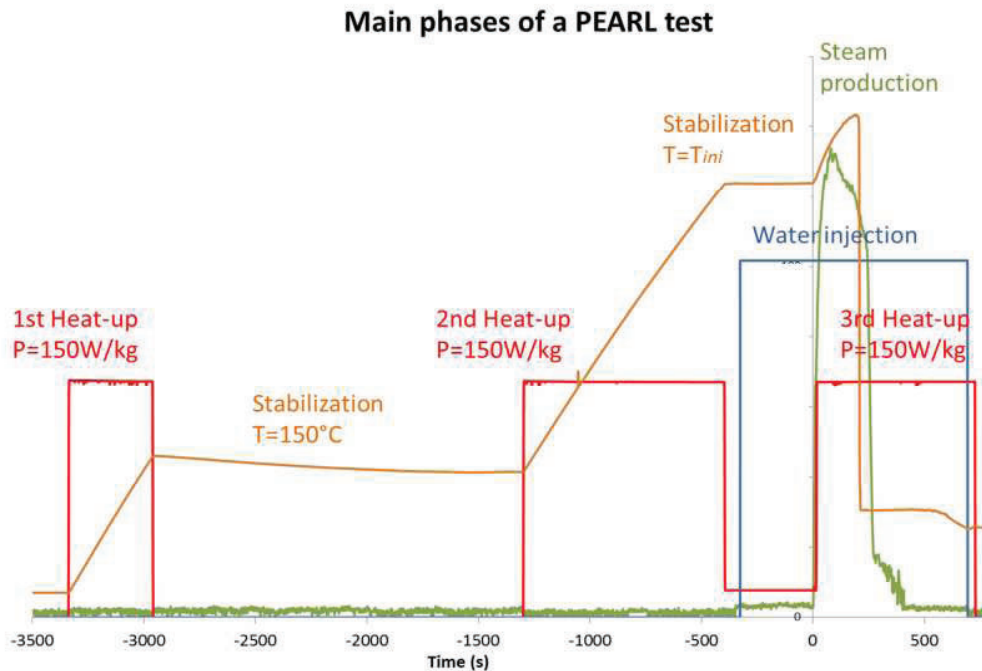


Figure 3. PEARL test conduct

2.4. Instrumentation and uncertainty

The main physical variables for model qualification are measured in the PEARL facility:

- Injected water and steam mass flow rate generated during reflooding,
- Temperature of the steam,
- Temperature inside the debris,
- Pressure at different points in the debris and at the boundaries of the debris bed.

The debris bed is equipped with K-type thermocouples (\varnothing 1 mm) located in the bed pores at different elevations (every 50mm) and radial and angular positions. The theoretical positions are given in the Fig.4. Exact positions have been determined after bed set up. The thermocouple nomenclature is as follow: TC-H-R- θ , H=height, R= radius and θ =angular. The steam temperature is also measured at the bed top exit and in the outlet steam line.

Absolute pressure is measured at the top of the test section. Six differential pressure transmitters are inserted into the bed (4) and into the bypass (2) to measure the pressure drop during reflooding for single or two-phase flows.

The water injection flow rate is measured by a Coriolis flow meter and controlled by an electro-pneumatic valve. The steam flow rate is measured with an Annubar flow meter. This flow meter consists of an absolute and a differential pressure sensor, and converts a pressure drop into fluid velocity.

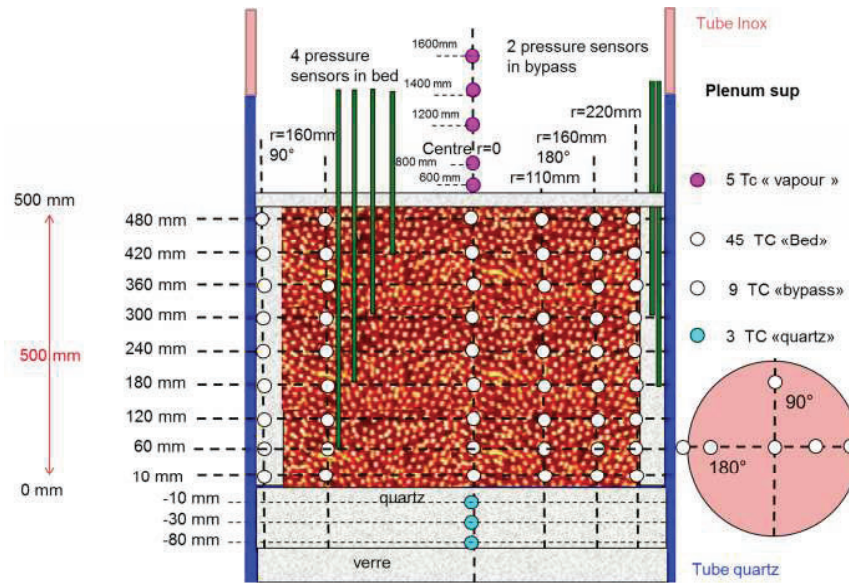


Figure 4. PEARL test section and thermocouple positions

Table I. Instrumentation and uncertainty

	Description	Range	Accuracy
Temperature	K-Type	-200/1100°C	±6.5°C
Differential Pressure	Rosemount 3051S2	-622/622 mbar	± 1,74 mbar
Absolute pressure	Rosemount 3051S2	0-12 bar	± 0,02 bar
Water flow rate	Emerson Coriolis	0-2000 g/s	±6 g/s
Steam flow rate (Annubar)	Rosemount 3051S1	0-12 bar	± 0,02 bar
	Rosemount 3051S3	-622/622 mbar	± 0,84 mbar

2.5. Induction heating

The experimental bed is heated with a 200kW induction furnace. The single induction coil is connected to a high frequency generator 100-400 kHz.

To heat homogeneously such a large bed is a challenging issue as the power would be preferentially concentrated in the peripheral area of the bed. For this reason, a specific treatment has been applied to all the stainless steel balls so that they are electrically insulated from each other. Then, the induced current is contained in each ball providing a volumetric distribution of the power.

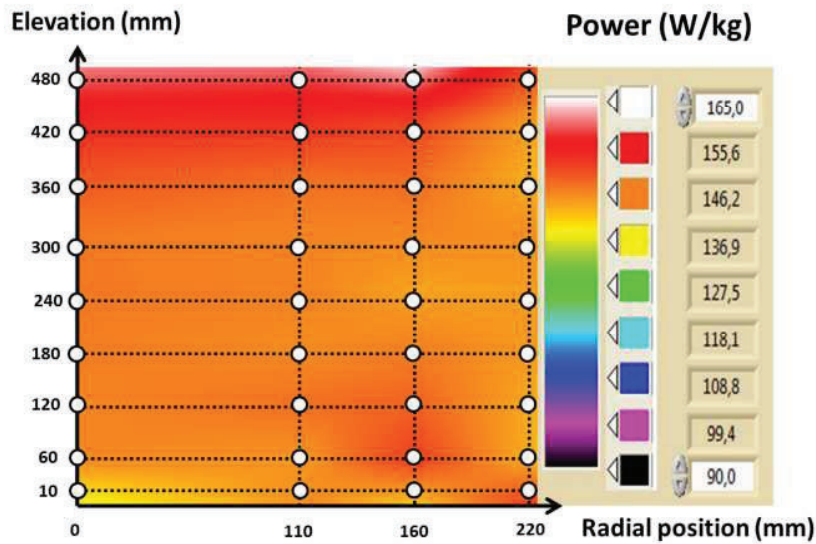


Figure 5. Power distribution – PEARL PA_2 Test

For each PEARL test, the power distribution has been determined according to the 42 thermocouples in the bed:

$$P(W / kg) = \frac{\partial T}{\partial t} * Cp \quad (1)$$

The calculation is done in the first seconds of the heating phase, when the heat losses can be neglected: when the bed is at room temperature, the temperature increases only due to the induction power deposit. Then, for each thermocouple of the bed, the power deposit is calculated when the bed temperature increased from 15°C to 25°C. It gives a series of 42 values. For the PEARL test PA_2 (Fig.5), the mean power is equal to 149W/kg and the standard deviation is equal to 9W/kg, i.e. 6% of the average value. The power distribution is practically homogenous in all the debris bed.

3. PEARL TEST RESULTS

3.1. Experimental results

Table II presents the first reflooding tests that have been performed in the PEARL facility. The effects of initial temperature, ranging from 150°C to 700°C, and the water injection velocity ranging from 2m/h to 10m/h, have been investigated.

Table II. PEARL test matrix

Test n°	Initial temperature (°C)	Injection flowrate (g/s) - velocity (m/h)	Power (W/kg)	Pressure (bar)
PA_0	150	318 - 5	150	1
PA_1	400	318 - 5	150	1
PA_2	700	318 - 5	150	1
PA_4	400	127 - 2	150	1
PA_5	400	635 - 10	150	1

For each test, the debris bed has been cooled down by water injection. The reflooding time is given in Table III. During the quench phase, the heating power has been maintained so that the dry part of the bed has continued to heat-up. That is why the maximum temperature reached in the bed during the test is higher than initial bed temperature (Table III). To illustrate this observation, the evolution of the debris bed temperature along the central axis during the PEARL PA_2 test is given in Fig. 6a. The typical temperature evolution can be divided in three steps. First, the bed is dry and submitted to steam convection, and its temperature increases due to the power deposit. Second, the quench front approaches the thermocouple position and the bed is cooled down by a steam-water flow, to the saturation temperature within few seconds. Finally, the bed remains at the saturation temperature and nucleate boiling occurs until the bed temperature decreases.

Table III. Reflooding time, Maximum temperature and cumulated steam production

Test n°	Reflooding time (s)	Temperature Max.	Steam production (kg)
PA_0	108	173	11.2
PA_1	240	447	30.7
PA_2	490	790	59
PA_4	440	490	44
PA_5	185	430	27.6

The quench front progression has been determined according to the temperature measurement. It is assumed that the quench front has reached a thermocouple position when its temperature falls down to the saturation temperature. This method is quite accurate because the quenching phase is very rapid with respect to the reflooding time: the bed temperature drops by hundreds of Celsius degrees within few seconds. The Fig. 6b gives the quench front progression during the PEARL PA_2 test, for several vertical axes in the bed. The quench front velocity can also be deduced from the temperature measurements. The mean quench front velocity (Table IV) ranges from 1 to 4.35mm/s. For tests PA_0 and PA_5, the quench front velocity in the by-pass is not available. Actually, the by-pass is not heated directly by the induction furnace as it is made of quartz balls, but indirectly by conduction due to the contact between steel balls and quartz balls. In the PA_0 test, the initial bed temperature is low (150°C). Thus, the initial by-pass temperature is equal to the saturation temperature and it is not possible to detect the quench front. In the PA_5 test, the injection flow rate is high (10m/h) so that the water rapidly flows from the water tank to the experimental bed. The conduction heating was too slow to heat the bypass over the saturation temperature and the quench front could not be detected.

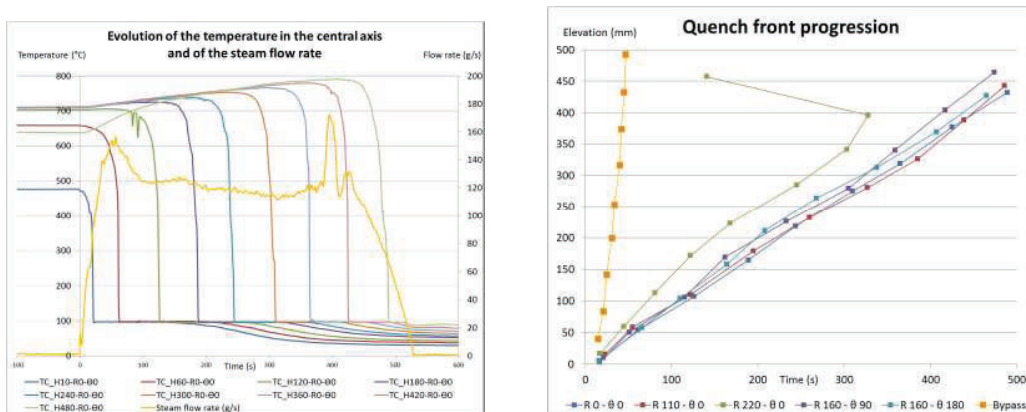


Figure 6. PEARL PA_2 test: a) Temperature evolution along the central axis, steam flow rate b) Quench front progression

In PA_1, PA_2 and PA_5 tests, the bypass was cooled faster than the experimental bed. For the PA_5 test, it can be seen on the video record. Thus, there was water accumulation on the top of the bed before the bed is totally quenched. Nevertheless, it did not cause top flooding. The external part of the bed (R=220mm) is cooled slightly faster than the central part (R=0→160mm) but the radial penetration of water is limited. The main penetration mode was the axial mode, bottom to top. The quench front area is quite flat in most part of the bed.

In the PA_0 and PA_4 tests, the bypass was cooled together with the rest of the bed and also played a minor role. Again, the reflooding was mainly driven from the bottom to the top.

Table IV. Quench front velocities

Quench front velocity (mm/s)	Axis R=0 θ=0	Axis R=110 θ=0	Axis R=220 θ=0	Axis R=160 θ=90	Axis R=160 θ=180	Average	Standard deviation (%)	Bypass
PA_0	4.18	4.36	4.36	4.57	4.31	4.35	3.2	NA
PA_1	2.09	2.08	2.60	2.07	2.01	2.17	11	7.30
PA_2	0.90	0.92	1.22	1.01	0.94	1	13	14.2
PA_4	0.99	1.02	1.11	1.07	1.03	1.04	4.7	1.25
PA_5	2.36	2.55	2.75	2.49	2.41	2.51	6.0	NA

The steam flow rate, produced during the tests, has been measured in the outlet steam line (Fig. 7). Two boiling regime phases can be distinguished for PA_0 and PA_4 tests. In the first phase, there is an increasing steam production up to approximately 80g/s due to the bed quenching and corresponding to the critical boiling. During the second phase, the steam production is significantly lower and corresponds to the moderate nucleate boiling while the bed is at the saturation temperature.

For PA_2 and PA_5 tests, the evolution of steam production is different. It starts with a “peak” of respectively 160g/s and 180g/s followed by a plateau and finished with a peak of same magnitude than the first one. The nucleate boiling cannot be clearly observed. As said earlier, water rapidly arrives on the top of the bed in these tests and an important part of steam was certainly condensed in this layer of water. The first peak is due to the first wetting of the bottom of the bed. The final peak is more difficult to interpret.

During the PA_1 test, the steam flow rate increased quickly to a maximum of 130g/s at the reflooding start and decreased slowly. The nucleate boiling is observed at the end of the test.

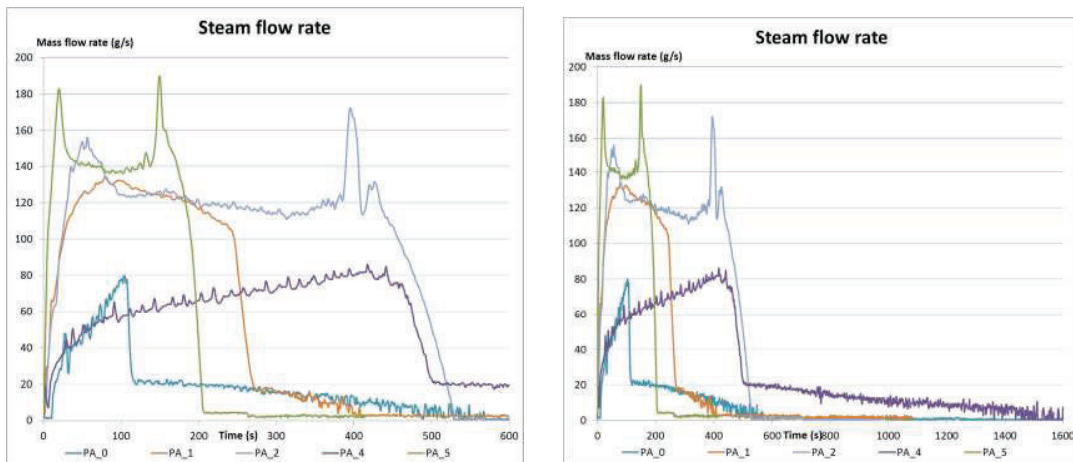


Figure 7. Steam flow rate

For each test, the water-steam conversion rate has been drawn in Fig. 8. The curve trends are also the same than for steam flow rate as the injection flow rate is constant (Fig. 7). For PA_0 and PA_4 tests, the conversion rate increased from resp. 10% and 30% to resp. 25% and 65%. The conversion rate is nearly constant and approximately equal to 40% in the PA_1 and PA_2 tests. For PA_5 test, the conversion rate is quite constant equal 22% (except for the peaks).

The conversion rate increases together with the initial temperature and decreases with the injection velocity.

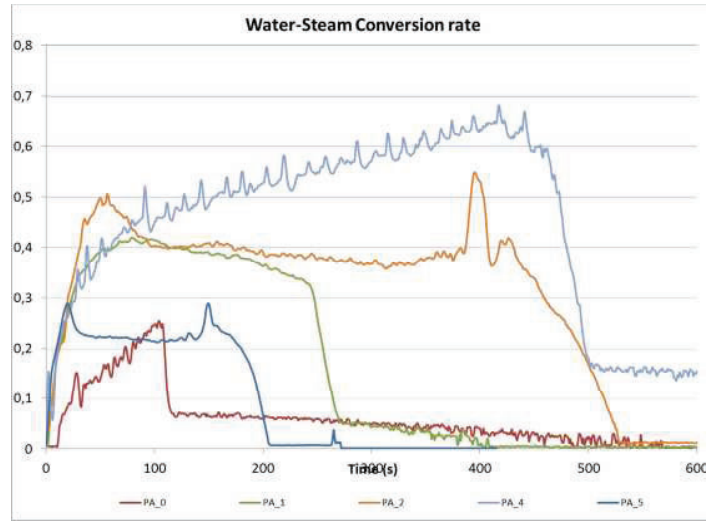


Figure 8. Steam-water conversion rate

3.2. Discussion

The effects of water injection velocity and initial bed temperature on the reflooding time have been investigated (Fig. 9). The quench front velocity decreases together with the injection flow rate. It is worth noticing that the reflooding time reduction is significantly higher when the injection flow rate is increased from 2 to 5 m/h than when it is increased from 5 to 10 m/h. It seems that the reflooding time tends to a limit value that cannot be reduced whatever the flow rate. This observation has already been done according to the PRELUDE reflooding tests performed on smaller bed (50kg, [19]).

The reflooding time increases with the initial temperature. The relation between initial temperature and the reflooding time is nearly linear. The main mode of energy removal is the latent heat of evaporation which is quite constant during the test. As the reflooding time is quasi proportional to the ratio of the initial energy (or initial temperature) to the latent heat, it is also proportional the initial temperature. It means that the power deposited during the test does not play an important role in these test conditions.

The reflooding time is shorter in PA_1 test ($T_{ini} = 400^{\circ}\text{C}$) than in PA_2 test ($T_{ini} = 700^{\circ}\text{C}$). The quench front velocities are respectively equal to 2.17mm/s and 1mm/s. And yet, the quench front velocity in the bypass is higher in PA_2 test (14mm/s) than in PA_1 test (7mm/s).

Moreover, these quench front velocities in the bypass are greater than the calculated value of the water front velocity which would happen in the case of a cold filling (5m/h) of the test section. According to the mean bed porosity (42%), the apparent water front velocity would be equal to 3.3mm/s.

Several conclusions can be drawn from these observations. First, during quenching, water is probably accelerated by steam in the bypass: it is a consequence of the interfacial drag force between steam and water in the hot porous medium. Second, the preferential exit path for steam is the bypass. Thus, the

steam generated in the debris bed makes a detour via the bypass, despite the presence of water, and, instead of going directly to the top of the bed. Actually, there is an important contrast of permeability between the experimental bed made of 4mm balls and the bypass made of 8mm balls. Then, pressure drops are lower in the bypass. It could explain such a behavior.

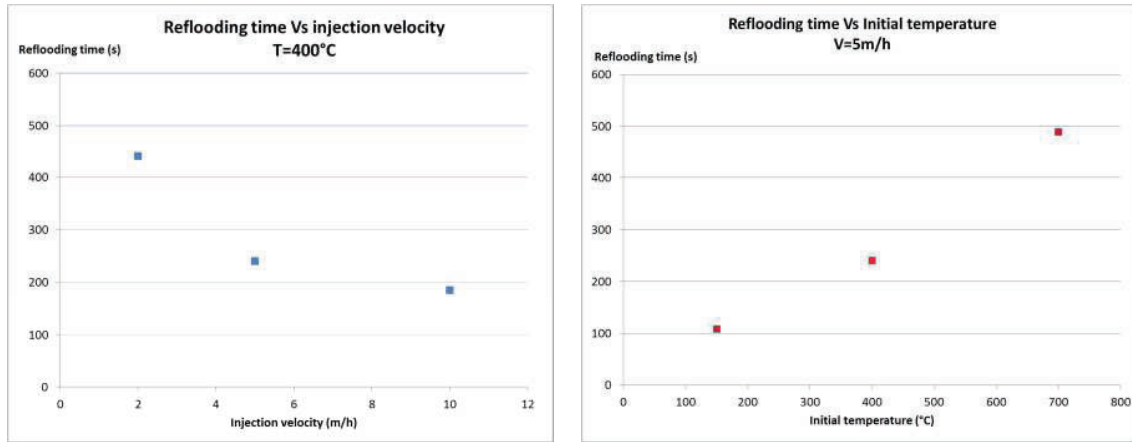


Figure 9. Effects of injection velocity and initial temperature on reflooding time

Finally, both water and steam flow preferentially through the bypass as it is colder and more permeable. It is true during the major period of reflooding, but no more true for steam at the end of reflooding. Actually, when only the central upper part of the debris bed remains dry, the steam generated at quench front can exit directly by the top of the experimental bed. Then, even if the experimental bed is less permeable than the bypass, the path to exit becomes so short that the pressure losses are lower in the debris bed than in the bypass (Fig. 10).

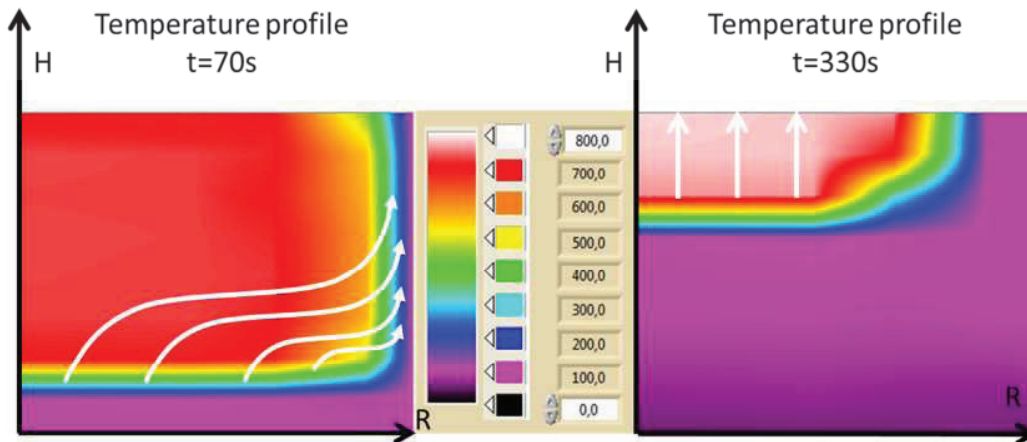


Figure 10. Steam trajectory during PEARL PA_2 test

This could explain the second steam peak observed in PA_2 and PA_5 tests. A part of steam could be condensed in the bypass during the plateau of steam production. Condensation should end when the steam exits straightly by the top of the bed.

Another interesting point is the quench front velocity in the PA_0 test (4.35mm/s) which is higher than the water front velocity (3.3mm/s, see above). It means that water flows more rapidly in a hot debris bed than in a cold one. In the PA_0 test, the quench front progression should have been limited by the bed

temperature and even more by the fact that part of water is evaporated. This phenomenon may be due to water swelling under the quench front: the presence of bubbles in the debris bed causes a water section reduction that could increase water velocity.

4. INTERPRETATION

4.1. Modelling

Analyzing the PEARL experimental results, it can be concluded, that there exists a quasi steady-state propagation of the quench front for all the cases considered here. This is exhibited by the quasi constant quench front velocity and the quasi-constant steam production rate. It indicates that the dynamic processes occurring in the bed are “fast” with respect to the injection velocity (no significant delay of quenching) but “stable” (no acceleration or dramatic increase of steam production). There are two noticeable events which show a different behavior: a peak of steam flow rate may occur at the beginning and at the end (in some tests). Those events result from transient effects when the quench front enters the superheated debris bed and when it exits the bed. However, during most of the propagation of the quench front, the behavior is quasi-steady. This had already been observed in PRELUDE experiment [14,15] but, in PRELUDE, the height of the bed was only 20cm and the relative effect of transient phases was more important, therefore it was less obvious to identify the quasi-steady behaviour in some cases. The quasi-steady steam production rate was already observed by Tutu et al. [3] and Tung and Dhir [6]. Those authors had proposed an expression of the conversion factor, i.e. the ratio between the steam flow rate and the water injection rate.

In this paper, following a similar approach for the interpretation of PEARL experiments, an updated model is proposed. It includes two specific features of the PEARL experiment, which are also relevant for a debris bed in a reactor: the residual power and the presence of a by-pass surrounding the debris bed. The model provides two main outputs: the steam conversion rate and the quench front velocity.

The development of the model is made in two steps: first, the quasi-steady propagation of the quench front in a uniform debris bed is considered, without by-pass (1D model) and, second, corrections are introduced to the model when a by-pass is present.

From the observations made in PRELUDE and PEARL, as well as in other experiments, it is reasonable to represent the flow in a simplified way, distinguishing three parts: a cold part ($T \leq T_{sat}$) where there is mostly water and possibly some steam due to volumetric power (depending on the degree of subcooling), a two-phase region where most of the cooling of particles occurs and finally a zone where only steam is present and where there is almost no cooling observed. This is represented in Fig. 11. It is assumed that the boundaries separating the different zones all move at the same velocity U_q .

From that representation, one may write two balance equations for the two-phase zone between z_1 and z_2 . First, the mass balance equation for the fluid (which is written in the relative frame moving at velocity U_q):

$$\rho_g (u_g(z_2) - U_q) = \rho_l (1 - \alpha(z_1))(u_l(z_1) - U_q) + \rho_g \alpha(z_1)(u_g(z_1) - U_q) \quad (2)$$

Second, the energy balance equation for the whole system (which is also written in the relative frame moving at velocity U_q):

$$\begin{aligned} \varepsilon \rho_g (u_g(z_2) - U_q) (h_g^{sat} + Cp_g \Delta T_g) - (1 - \varepsilon) \rho_s U_q Cp_s \Delta T_s = \\ \varepsilon \rho_l (1 - \alpha(z_1))(u_l(z_1) - U_q) h_l^{sat} + \varepsilon \rho_g \alpha(z_1)(u_g(z_1) - U_q) h_g^{sat} \end{aligned} \quad (3)$$

Introducing the first balance equation into the second one in order to eliminate the unknown outlet velocity of steam $u_g(z_2)$, one gets:

$$U_q [\varepsilon \rho_l (1 - \alpha(z_1)) (\Delta h^{sat} + C p_g \Delta T_g) + \varepsilon \rho_g \alpha(z_1) C p_g \Delta T_g + (1 - \varepsilon) \rho_s C p_s \Delta T_s] = \varepsilon \rho_l (1 - \alpha(z_1)) u_l(z_1) (\Delta h^{sat} + C p_g \Delta T_g) + \varepsilon \rho_g \alpha(z_1) u_g(z_1) C p_g \Delta T_g \quad (4)$$

Simple mass and energy balance in the bottom zone, between z_0 and z_1 , gives the values of $(1 - \alpha(z_1)) u_l(z_1)$ and $\alpha(z_1) u_g(z_1)$ at the entrance of the quenching zone:

$$\rho_l (1 - \alpha(z_1)) u_l(z_1) + \rho_g \alpha(z_1) u_g(z_1) = \rho_l u_l^0 \quad (5)$$

$$\alpha(z_1) u_g(z_1) = \frac{\dot{Q}_s}{\varepsilon \Delta h^{sat}} (z_1 - z_0) \quad (6)$$

From those equations, the quench front velocity U_q is derived:

$$\gamma_u = \frac{U_q}{u_l^0} = \frac{\varepsilon \rho_l (\Delta h^{sat} + C p_g \Delta T_g) - \rho_g \dot{Q}_s \gamma^* t}{\varepsilon \rho_l (1 - \alpha(z_1)) (\Delta h^{sat} + C p_g \Delta T_g) + \varepsilon \rho_g \alpha(z_1) C p_g \Delta T_g + (1 - \varepsilon) \rho_s C p_s \Delta T_s} \quad (7)$$

The mass flow rate of steam produced is then obtained with:

$$\rho_g u_g(z_2) = \rho_l u_l^0 - U_q (1 - \alpha(z_1)) (\rho_l - \rho_g) \quad (8)$$

From, that, the conversion rate is obtained

$$\gamma_q = \frac{\rho_g u_g(z_2)}{\rho_l u_l^0} = 1 - \gamma_u (1 - \alpha(z_1)) \left(1 - \frac{\rho_g}{\rho_l}\right) \quad (9)$$

4.2. Application to the PEARL test

The model is now applied to the PEARL tests presented in the previous sections.

The direct application of the model provides the following conversion factors, shown in Fig. 12.

It can be seen that some conversion ratios are rather well predicted when the injection flow rate is low or when the temperature of the bed is low (PA_0 and PA_4 tests). If the temperature is higher or the injection velocity is higher, the conversion ratio is over predicted. This may indicate that the increase of steam production leads to a deviation of a part of the injected liquid into the by-pass, where it is not converted into steam and flow up to the top of the particle bed, as observed in the temperature measurements in the by-pass (Fig.10).

In Fig. 12, and in particular for the PA_0 and PA_4 tests, the conversion ratio is clearly seen to increase during the experiment. This is a direct consequence of the volumetric power and the fact that there is an increasing amount of steam injected at the quench front as the quench front position moves upwards. Such result was less obvious in PRELUDE experiments because of a much lower height of the bed (only 20 cm).

The effect of deviation of a part of the inlet flow into the bypass is also clearly seen in PA_5 test and, to a lesser extent, in PA_2 test. In those tests, the conversion ratio is significantly lower than it would be without the bypass. This will be discussed in subsection 4.3.

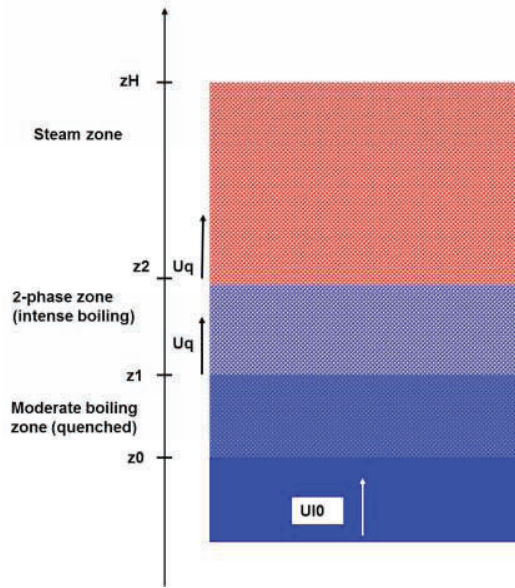


Figure 11. 1D-modelling of the quench front during quasi-steady progression, without by-pass

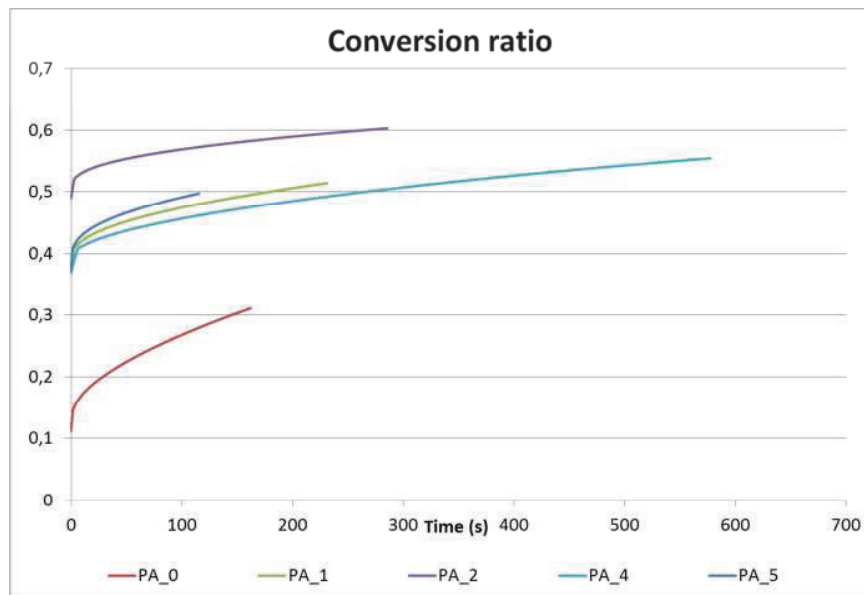


Figure 12. Conversion ratios predicted by the 1D model

The velocities of quench front predicted by the model are compared to the measurements in Table V. For 3 tests (PA_1, PA_2, PA_4), it is predicted with a relative error lower than 20%. Significant discrepancies are observed for cases PA_0 (underprediction) and PA_5 (overprediction). One possible explanation for the case PA_0, with low superheat of the particles, would be the predominant effect of volumetric power leading to swelling of water below the quench front and an apparent velocity of water at the quench front greater than the injection velocity. For PA_5 test, the quench front velocity is significantly overpredicted. The explanation for the discrepancy is not obvious but it may be due to a rather strong entrainment of water in the bypass leading to an “apparent injection velocity” lower than the real one. This will have to be investigated further.

Table V. Quench front velocities measured and calculated

Quench front velocity (mm/s)	Measured	Modelled	Possible explanation for discrepancy
PA_0	4.35	3.1	Boiling below the quench front induces a swelling velocity greater than the injection velocity
PA_1	2.17	2.2	-
PA_2	1	1.3	-
PA_4	1.04	0.86	-
PA_5	2.51	4.5	Possible effect of entrainment of water in the by-pass

4.3. Discussion on the consequences of entrainment of water in the by-pass

The discrepancies obtained from the previous analysis shows that an important process occurring because of the presence of the by-pass was not taken into account. This process is probably the entrainment of water in the by-pass. Several experimental observations tend to prove that a significant amount of water may be entrained in the by-pass. First, in the movies made during the tests, it was clearly seen that, in some cases, water arrives on top of the bed before the bed is fully quenched. Second, the measured quenching velocity in the by-pass is much higher than the quench front velocity in the main bed, indicating that some water flows rapidly in the by-pass.

The only physical explanation for the progression of water in the by-pass, at a velocity larger than quench front velocity is the entrainment by steam, through interfacial friction. If the formalism of the generalized Darcy-Forscheimer momentum equations for the two-phase flow is used, the velocity of the liquid phase can be estimated by identifying the pressure gradients in the liquid and gas phases:

$$\frac{\partial P}{\partial z} = -\rho_l g + \frac{\mu_l}{KK_{rl}} u_l = -\rho_g g + \frac{\rho_g}{\eta\eta_{rl}} u_g^2 \quad (10)$$

In the previous equation, the Ergun (i.e. quadratic) term was neglected in the liquid phase equation because of the low Reynolds number and, conversely, the Darcy (i.e. linear) term was neglected in the gas phase equation because of the large Reynolds number. This gives the liquid phase velocity:

$$u_l = \frac{KK_{rl}}{\mu_l} \left(-(\rho_l - \rho_g)g + \frac{\rho_g}{\eta\eta_{rl}} u_g^2 \right) \quad (11)$$

From that equation, a necessary condition for entrainment of water can be derived: the liquid velocity in the by-pass must be positive. Otherwise, water in the by-pass falls down into the main debris bed, from the lateral boundary. A similar criterion was found in PRELUDE to determine the existence of 2D effects [16]. This condition is represented in Fig. 13 but, in order to estimate it quantitatively, one has to evaluate the gas velocity in the by-pass. This may be done by assuming that vertical pressure gradients are equal in the by-pass and in the main bed, and that the total gas flow is given by the conversion ratio, from the model developed in subsection 4.1:

$$\frac{\partial P}{\partial z} = \frac{\rho_g}{\eta_1} u_{g1}^2 = \frac{\rho_g}{\eta_2} u_{g2}^2 \quad (12)$$

$$\rho_g (S_1 u_{g1} + S_2 u_{g2}) = \gamma_q \rho_l (S_1 + S_2) u_{l0} \quad (13)$$

This gives the gas velocity in the by-pass which is used to evaluate the criterion for water entrainment shown in Fig. 14 (left).

$$u_{g2} = \gamma_q \frac{\rho_l}{\rho_g} \frac{1}{S_2} \left(1 + \frac{S_1 \eta_1^{0.5}}{S_2 \eta_2^{0.5}} \right)^{-1} \quad (14)$$

One can see that PA_2 and PA_5 tests are well above the criterion which means that a significant fraction of the inlet flow is likely to be entrained in the by-pass and would not contribute to the quenching of the main bed. The case PA_1 is also above the criterion but not much and, considering the assumptions and approximations made, it is not obvious to conclude about the water entrainment in that case.

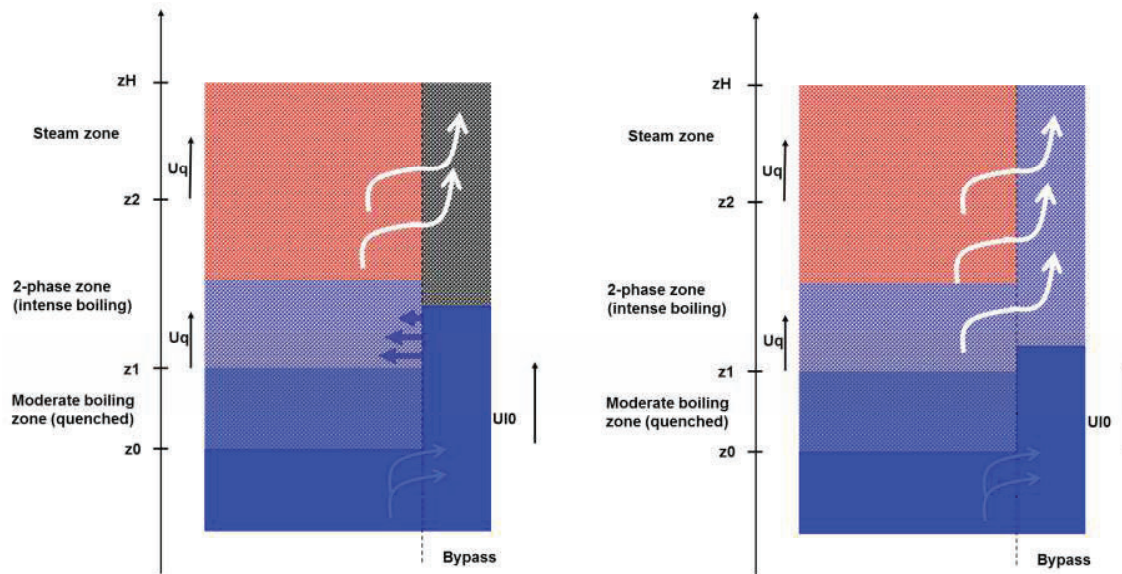


Figure 13. 2D-modelling of the entrainment of water in the by-pass – left: diverted steam flow is insufficient to entrain water, water from the by-pass flows into the main bed – right: diverted steam flow is sufficient to entrain water, water in the by-pass flows towards the top and does not contribute to cooling of the main bed

In order to check the effect of water entrainment, the 1D model is modified, assuming that the excess water flowing in the bypass cannot enter the superheated debris bed because it is entrained by steam produced. Then, in the balance equation (2) and (3), the inlet water flow at the bottom boundary z_1 is reduced according to the section of the experimental bed instead of the whole test section:

$$\rho_g (u_g(z_2) - U_q) = \frac{S_1}{S_1 + S_2} \rho_l (1 - \alpha(z_1))(u_l(z_1) - U_q) + \rho_g \alpha(z_1)(u_g(z_1) - U_q) \quad (15)$$

The expression (9) for the conversion ratio is slightly modified and is written as:

$$\gamma_q = (1 - \gamma_u)(1 - \alpha(z_1))S_1 - S_2 / (S_1 + S_2) \quad (16)$$

The results are presented in Fig. 14 (right) and it can be seen that, with this simple assumption, the conversion ratio for PA_2 test is significantly reduced and is in agreement with the experimental measurement. For PA_5 test, it is also reduced and the agreement is good too. In particular, it shows that, for a given initial temperature of the bed, the conversion ratio cannot be increased by increasing the injection velocity. There is a kind of “saturation” of the bed which cannot produce more steam as soon as the criterion for water entrainment is reached, leading to a constant conversion ratio after a threshold velocity. This would have to be confirmed by further tests and analysis.

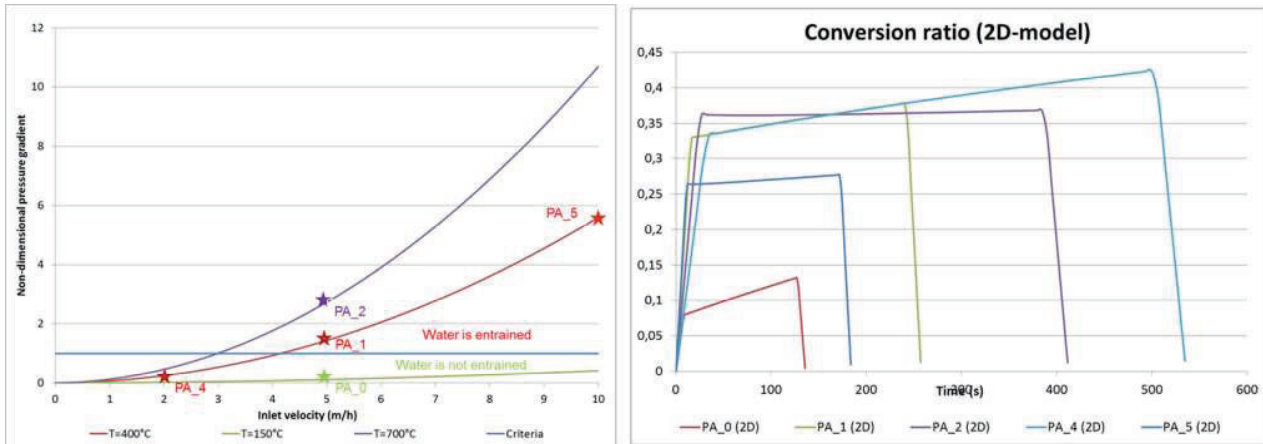


Figure 14. Evaluation of the conditions necessary for water entrainment in the by-pass (left) - Conversion factors predicted by the modified model taking into account entrainment of water for cases 2 and 5 (right)

5. CONCLUSION

The PEARL facility was design to perform reflooding tests on large scale debris beds in order to study degraded core coolability. Five reflooding tests have been carried out with an experimental bed, 500mm in height and 500mm in diameter, made of 4mm stainless steel balls. The initial bed temperature and the water injection velocity range were respectively from 150°C to 700°C and from 2m/h to 10m/h. For the first time, such a large bed was heated practically homogenously. The volumetric power, provided by an induction furnace before and during reflooding, was equal to 149W/kg \pm 6%. The steam generated during the reflooding was measured and the quench front velocity was determined according to thermocouple measurements inside the bed.

For each tests, the bed has been cooled down by water injection. The quench front progression was axial and homogenous in most of the bed ($R < 160$ mm). The bypass was cooled faster especially for high initial temperature and high injection velocity. Then, a layer of water was accumulated at the top of bed before the end of reflooding, but it did not cause top flooding. Steam generated at quench front exited the bed preferentially through the bypass entraining water. As a consequence, water was accelerated in the bypass. This phenomenon also limited the radial quench progression.

The effects of initial temperature and water injection velocity on the reflooding time have been investigated. The reflooding time is quasi proportional to the initial temperature, and it decreases together with the injection velocity. More, it seems that the reflooding time tends toward a lower limit. Tests performed with higher injection velocity would confirm this point.

An analytical model, assuming a quasi-steady progression of the quench front, allows to predict the conversion ratio in most cases. However, under some conditions (high injection velocity or high initial temperature of the debris bed), it is shown that a significant amount of injected water may be entrained in the by-pass and does not directly contribute to cooling of the particle bed. This reduces the conversion ratio. A modified model, taking into account that effect, provides better agreement with experimental measurements. This indicates that the basic processes of steam diversion and water entrainment in the by-pass have been correctly approximated with the proposed assumptions.

One of the most important conclusion of the first PEARL experiments is that the presence of a bypass around the debris bed leads to significantly different results compared to previously obtained data. The differences come from the limitation of the pressure gradient in the main debris bed, caused by the redistribution of steam in the by-pass. This redistribution may lead to water entrainment in the by-pass, reducing the flow of water into the main bed. As a result, it appears that the efficiency of cooling can be

increased only up to a certain limit when increasing the inlet water flow rate. As a perspective, a scaling analysis should be done to quantify applicability of the experimental configuration to reactor processes.

NOMENCLATURE

γ_q , conversion ratio of the injected mass flow rate

γ_u , ratio between quench front velocity and injection velocity

α , ratio void fraction

S , area of the section (m²): index 1 for the main (experimental) bed and 2 for the bypass

u , velocity (m/s)

ρ , density (kg/m³)

K , permeability (m²)

η , passability (m)

P , pressure (Pa)

z , elevation in the porous medium (m)

ACKNOWLEDGMENTS

This work was partially sponsored by Electricité de France (EDF) through a bilateral partnership with IRSN.

REFERENCES

1. J.M. Broughton, P. Kuan, D.A. Petti, and E.L. Tolman. "A scenario of the Three Mile Island unit 2 accident". *Nuclear Technology*, **87**, pp.34–53, 1989
2. D. Magallon. "The FARO program recent results and synthesis". In *Proceedings of CSARP Meeting, Bethesda, USA, May 1997*
3. R.J. Lipinski, "A coolability model for postaccident nuclear reactor debris". *Nuclear Technology*, **65** pp.53–66, April 1984
4. K. Atkhen and G. Berthoud. "Experimental and numerical investigations on debris bed coolability in a multidimensional and homogeneous configuration with volumetric heat source". *Nuclear Technology*, **142**, June 2003.
5. D.R. Armstrong, D.H. Cho, L. Bova, S.H. Chan, and G.R. Thomas. "Quenching of a high temperature particle bed". *Transactions of the American Nuclear Society*, **39** pp.1048–1049, 1981
6. D.H. Cho, D.R. Armstrong, and S.H. Chan. "On the pattern of water penetration into a hot particle bed", *Nuclear Technology*, **65** pp.23–31, 1984.
7. T. Ginsberg, J. Klein, J. Klages, Y. Sanborn, C.E. Schwarz, J.C. Chen, and L. Wei. "An experimental and analytical investigation of quenching of superheated debris beds under top-reflood conditions", Technical Report NUREG-CR-4493, Brookhaven National Labs., 1986
8. N.K. Tutu, T. Ginsberg, J. Klein, J. Klages, and C.E. Schwarz. "Debris bed quenching under bottom flood conditions", Technical Report NUREG/CR-3850, Brookhaven National Labs., 1984.
9. M.J. Konovalikhin, Z.L. Yang, M. Amjad, and B.R. Seghal, "On dry-out heat flux of particle debris beds with a downcomer", In *Proceedings of ICONE 8, 8th International Conference on Nuclear Engineering, Baltimore (USA), April 2000*.
10. F. Petit, F. Fichot, and M. Quintard. « Ecoulement diphasique en milieux poreux : Modèle à non équilibre local », *Int. J. Therm. Sci*, **38** pp.239–249, 1999
11. M. Sozen and K. Vafai. "Analysis of the nonthermal equilibrium condensing flow of a gas through a packed bed", *Int. Journal of Heat and Mass Transfer*, **33**(6) pp.1247–1261, 1990.
12. V.K. Dhir and G.P. Purohit. "Subcooled film boiling heat transfer from spheres", *Nuclear Engineering and Design*, **47** pp.49–66, 1978.
13. F. Duval, F. Fichot, and M. Quintard, "A local thermal non-equilibrium model for two-phase flows with phase change in porous media", *International Journal of Heat and Mass Transfer*, **47**(3) pp.613–639, 2004.
14. Repetto G., Garcin T., Eymery S., March P. and Fichot F. : "Experimental program on debris bed reflooding (PEARL) – Results on PRELUDE facility", *Proceedings of NURETH-14 Conference, Toronto (Canada), 2011*
15. Fichot F., Bachrata A., Repetto G., Fleurot J. and Quintard M. : "Quenching of a highly superheated porous medium by injection of water", *J. Phys.: Conf. Ser.* Vol. 395, 2012
16. Bachrata, A., Fichot, F., Repetto, G., Quintard, M. and Fleurot, J. : "Quench Front Progression in a Superheated Porous Medium: Experimental Analysis and Model Development", *Journal of Energy and Power Engineering*, Vol. 7, pp. 514-523, 2013
17. Magallon D. et al., "MFCI Project Final Report", *European Commission report INV-MFCI(99)-P007*, 1999
18. Kudinov, P., Karbojian, A., Weimin, Ma., Dinh, T.-N.: "The DEFOR-S experimental study of debris formation with corium simulant materials", *Nuclear Technology*, 170 (1), pp. 219-230, 2010
19. Repetto G., Chikhi N. and Fichot F. : "Main outcomes on debris bed cooling from PRELUDE experiments", *Proceedings of ERMSAR Conference, Avignon (France), 2013*